DNA Sequence-Specific Recognition by the *Saccharomyces cerevisiae* "TATA" Binding Protein: Promoter-Dependent Differences in the Thermodynamics and Kinetics of Binding†

Victoria Petri, Mark Hsieh, Elizabeth Jamison, and Michael Brenowitz*

Department of Biochemistry, Albert Einstein College of Medicine, 1300 Morris Park Avenue, Bronx, New York 10461

Received May 8, 1998; Revised Manuscript Received July 30, 1998

ABSTRACT: The equilibrium binding and association kinetics of the *Saccharomyces cerevisiae* TATA Binding Protein (TBP) to the E4 and Major Late promoters of adenovirus (TATATATA and TATAAAAG, respectively), have been directly compared by quantitative DNase I titration and quench-flow "footprinting". The equilibrium binding of TBP to both promoters is described by the equilibrium TBP + DNA$_{\text{"TATA"}}$ ↔ TBP−DNA$_{\text{"TATA"}}$. The salt dependence of TBP binding to both promoters is identical within experimental error while the temperature dependence differs significantly. The observed rate of association follows simple second-order kinetics over the TBP concentration ranges investigated. The salt and temperature dependencies of the second-order association rate constants for TBP binding the two promoters reflect the dependencies determined by equilibrium binding. The TBP−E4 promoter interaction is entropically driven at low temperature and enthalpically driven at high temperature while the TBP-Major Late promoter reaction is entropically driven over virtually the entire temperature range investigated. These data suggest that the reaction mechanisms of TBP-promoter interactions are TATA sequence-specific and provide for differential regulation of promoters as a function of environmental variables.

The "TATA binding protein" (TBP) is a component of the nucleoprotein complexes required for the initiation of transcription by each of the three eukaryotic RNA polymerases (*1*−*3*). The binding of TBP to specific promoter sequences called "TATA boxes" is a key step in the initiation of the transcription of genes transcribed by RNA polymerase II (*4*, *5*). The nucleotide sequence of TATA boxes is variable among naturally occurring promoters (*6*). The two promoters investigated in the present study, the adenovirus E4 (TATATATA) and Major Late (TATAAAAG) promoters, bind TBP with high affinity, are efficiently transcribed, and are among four high-affinity sequences identified by a selection protocol (*7*). Atomic resolution structures of TBP from several species, free (*8*−*11*) and complexed to DNA (*12*−*16*), have been solved to high resolution. The DNA within the TBP−promoter complexes is unwound, exposing a broad and flat minor groove to the protein that results in a DNA bend that follows a complex trajectory. The overall geometries of the TBP−DNA complexes are superimposable although local differences are observed in the conformations of, and interactions between, the bases and amino acids.

The temperature dependence of *Saccharomyces cerevisiae* TBP binding to the E4 promoter was shown to be characterized by a standard-state heat capacity change, ΔC_p°, on the order of −3 kcal/(mol K) (*17*). This highly negative value of ΔC_p° could not be rationalized by the simple burial of nonpolar surface area (*18*) nor coupled protein folding (*19*) based upon the TBP and TBP−DNA structures cited above. The temperature dependencies of the equilibrium binding and association rate constants determined for the TBP−E4 interaction were the same within experimental error (*17*).

The DNA association kinetics of *S. cerevisiae* TBP are second-order with TBP (*17*, *20*−*22*). A diffusion-limited intermediate was not observed in the course of the association reaction in stopped-flow experiments conducted with dead times as short as several milliseconds (*21*, *22*). The fluorescence resonance energy transfer (FRET) stopped-flow kinetics studies further demonstrated that the TBP-induced DNA bend occurred simultaneously with the formation of the TBP−DNA complex (*22*). These data are inconsistent with a reaction mechanism where the diffusion rate-limited binding of TBP to DNA results in the formation of a stable "encounter complex" that slowly isomerizes to the final bent TBP-DNA complex (*17*, *21*, *22*). Rather, the "slow binding" of TBP is predicted to result from the small number of TBP−DNA collisions that form a productive chemical complex. The transient encounter complex is not detectable due to its very low steady-state concentration and a large activation barrier that must be overcome for it to proceed along the reaction pathway. If this barrier results from a DNA conformational change, then the slow rate of DNA binding by TBP would derive from TBP sampling the distribution of rapidly equilibrating DNA conformers for the small fraction to which it can productively bind (*22*). This hypothesis suggests that TBP−DNA association kinetics will be DNA sequence-dependent.

The studies presented in this paper demonstrate differences in the thermodynamics and kinetics of TBP binding to two promoters that are efficiently transcribed by RNA polymerase II. The temperature and salt dependencies of the association

† These studies were supported by Grants GM51056, GM39929, F31-GM13850 (M.H.), and 5T32-GM07491 (V.P.) from the National Institutes of Health and by the Hirshl Weill-Caulier Trust.

* To whom correspondence should be addressed.

10.1021/bi981072u CCC: $15.00
Published on Web 10/20/1998

rates reflect those of the equilibrium binding constants for both promoters although the temperature dependence of the Major Late promoter is reduced compared to the E4 promoter. Comparison of these dependencies for the binding thermodynamics and kinetics suggests that the transition state detectable by DNase I footprinting for the TBP−DNA binding reaction has appreciable character of the final complex.

EXPERIMENTAL PROCEDURES

Protein and DNA. The 789 bp *Afl*III/*Sap*I restriction fragment containing the *adenovirus* Major Late promoter was excised from plasmid pM_LC_2AT (*23*). The 334 bp *Hind*III/*Eco*R1 restriction fragment containing the *adenovirus* E4 promoter was excised from plasmid pE_4T that was a gift of Dr. Stephen Triezenberg. *S. cerevisiae* TBP was expressed and purified as described (*17*, *22*). The TBP preparation used in these studies was fully active in sequence-specific DNA binding. The preparation of the ^{32}P-DNA restriction fragments used in the footprinting assays has been described previously (*17*).

Equilibrium and Kinetic "Footprinting". DNase I footprint titration experiments were conducted as described (ref *17* and references therein). A detailed protocol for the kinetics quench-flow DNase I footprinting assay has been published (*24*). The buffer used in the binding reactions contains 25 mM Bis-tris, 5 mM $MgCl_2$, 1 mM $CaCl_2$, 100 mM KCl, 2 mM DTT, 1 μg/mL poly dG-dC, pH 7.4 at the indicated temperature. All reagents and solutions were equilibrated for >45 min at the indicated temperatures prior to initiation of the footprinting reaction. Both the equilibrium and kinetic studies were conducted under conditions where [TBP] ≫ [DNA] ([DNA] = 1−10 pM), enabling the assumption that $[TBP]_{total} \approx [TBP]_{free}$ to be made in the analysis of the data. The electrophoresis gels were imaged using a Molecular Dynamics phosphorImager.

Quantitation of the digital images was conducted using the ImageQuant (Molecular Dynamics) software as described elsewhere (*25*, *26*). Fractional saturation ($\bar{Y}$) of the TATA box was determined from the fractional protection (p_i) of bands visualized on the PhosphorImager by nonlinear least-squares fitting of the data against

$$p_i = p_{i,lower} + (p_{i,upper} - p_{i,lower})\bar{Y} \quad (1)$$

where

$$\bar{Y} = \frac{K^{nH}[TBP]^{nH}}{1 + K^{nH}[TBP]^{nH}} \quad (2)$$

or

$$\bar{Y} = 1 - e^{-k_{obs}t} \quad (3)$$

for the equilibrium titration (eq 2) or kinetic progress (eq 3) curves, where p_i is the apparent saturation, $p_{i,lower}$ and $p_{i,upper}$ are the limits of the transition curves, K is the equilibrium association constant, n_H is the Hill coefficient (When n_H = 1.0, eq 2 reduces to the single-site binding expression.), k_{obs} is the pseudo-first-order rate constant, and t is time (*24*, *25*, *27*).

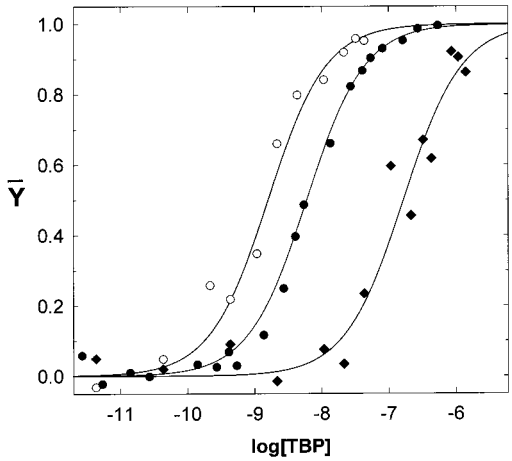

FIGURE 1: Binding isotherms obtained from "footprint" titration experiments of TBP binding to the Major Late promoter at 30 °C at 50 (○), 100 (●) and 200 (◆) mM KCl. The solid lines are the best fits to eqs 1 and 2 with $\Delta G° = -12.2 \pm 0.2$ kcal/mol, $n_H = 1.0 \pm 0.3$ (○), $\Delta G° = -11.3 \pm 0.1$ kcal/mol, $n_H = 1.1 \pm 0.2$ (●) and $\Delta G° = -9.4 \pm 0.2$ kcal/mol, $n_H = 1.0 \pm 0.3$ (◆). $\bar{Y}$ is the fractional saturation of the DNA binding site. [TBP] is the free concentration of TBP.

For a bimolecular association reaction, $k_{obs} = k_a[TBP] + k_d$ (*28*). Direct global fitting of the family of progress curves obtained as a function of [TBP] at each temperature was unable to resolve unique values of k_d (analysis not shown). Since at some temperatures the association kinetics data were sufficient to estimate $k_d \leq 0.01$ s^{-1}, each data set was refit with k_d fixed at this value; the values of k_a obtained from these fits were indistinguishable, within experimental error, from those obtained assuming that k_d was equal to 0 (data not shown).

Each data set was analyzed and scaled to use the best-fit limits (eq 1). When multiple data sets were globally analyzed, each data set was weighted by the inverse of the square root of the variance of its individual fit. To ensure that the errors in the binding measurements are propagated from the experimental data, the determination of $\Delta C_p°$, SK_{obs}, and Sk_{obs} was conducted by globally analyzing either the constituent binding isotherms or the kinetics progress curves against the appropriate expressions (*18*, *29*) as described (*17*).

RESULTS

Equilibrium Binding. TBP−Major Late promoter equilibrium binding isotherms shown in Figure 1 were obtained at 30 °C at 50, 100, and 200 mM KCl and are described by the Langmuir binding polynomial. This observation is general for both promoters over the temperature range investigated at 100 mM KCl. The dependence on [KCl] of the binding of TBP to the Major Late promoter is identical to that determined for the E4 promoter (Figure 2; Table 1) (*17*).

A van't Hoff plot depicting the equilibrium binding constants obtained at 100 mM KCl as a function of temperature for the E4 and Major Late promoters is shown in Figure 3. The $\Delta C_p°$ values obtained for the two promoters, determined from a global analysis of the constituent binding isotherms, differ by 1.8 kcal/(mol K) (Table 2), a value that greatly exceeds the confidence limits of the measurements. To confirm this difference, pairs of E4 and Major Late promoter binding reactions were simultaneously

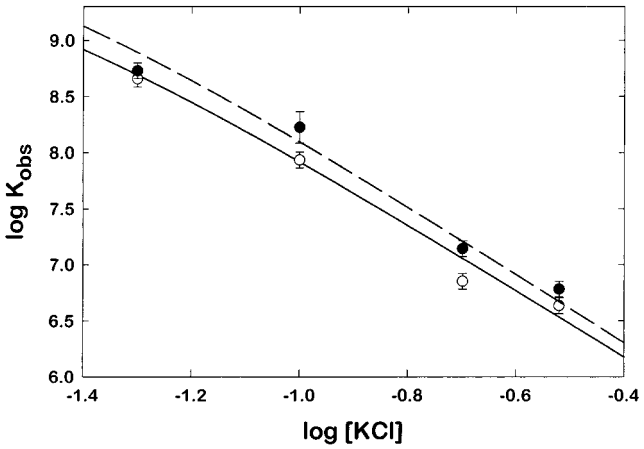

FIGURE 2: The salt dependence of the equilibrium binding of TBP with the Major Late (○) and E4 (●) promoters. The data were fit to the equations presented in ref *29* as described previously (*17*) by floating m and K_o at a fixed value of log $K_o^{2+} = -0.88$, previously determined (*17*) as the limiting value at which no further improvement of the fit was obtained. The results of the fits are shown in Table 1.

Table 1: The [KCl] Dependence of TBP Binding to the E4 and Major Late Promoters

promoter	SK_{obs}[a]	log $K_{obs,1\ M}$	$\sqrt{var}$
K_{eq}			
E4: TATATATA	-3.5 ± 0.3	5.1 ± 0.3	0.049
MLP: TATAAAAG	-3.4 ± 0.2	5.0 ± 0.2	0.017
promoter	Sk_a[a]	log $k_{obs,1\ M}$	$\sqrt{var}$
k_a			
E4	-2.7 ± 0.3	3.2 ± 0.3	0.156
MLP	-2.8 ± 0.2	3.3 ± 0.3	0.132

[a] $-Sk_{obs}$ and $-Sk_{obs}$ were calculated following ref *29* as described (*17*).

conducted at each temperature; the data shown in Figure 3 includes these direct comparisons.[1] Over the temperature range of 15−30 °C, the binding of TBP to both promoters is endothermic although somewhat less so for the Major Late promoter.

Association Kinetics. An example of a quench-flow DNase I kinetics footprinting experiment is shown in Figure 4. An advantage of the use of a rapid-mixing device in these experiments is that data over the entire course of the progress curve can be collected at hundreds of nanomolar TBP concentrations. The DNase I kinetics progress curves that have been obtained for the TBP−DNA binding reactions are described by a single exponential (eq 3); additional kinetic phases have not been discernible using the DNase I footprinting assay under the experimental conditions investigated. The rate of association of TBP with the Major Late and E4 promoters decreases with increasing [KCl] (Figure 5). The salt dependencies of k_a for the Major Late and E4 promoters determined from global analysis of the progress curves are identical within experimental error (Table 1). The Major Late promoter binds slightly faster at all the salt concentrations investigated, although this difference does not exceed

[1] The difference in the values of $\Delta C_p°$ determined for the E4 promoter herein and previously (*17*) does not exceed the errors in the determinations and is the result of the more extensive data set analyzed in the present study.

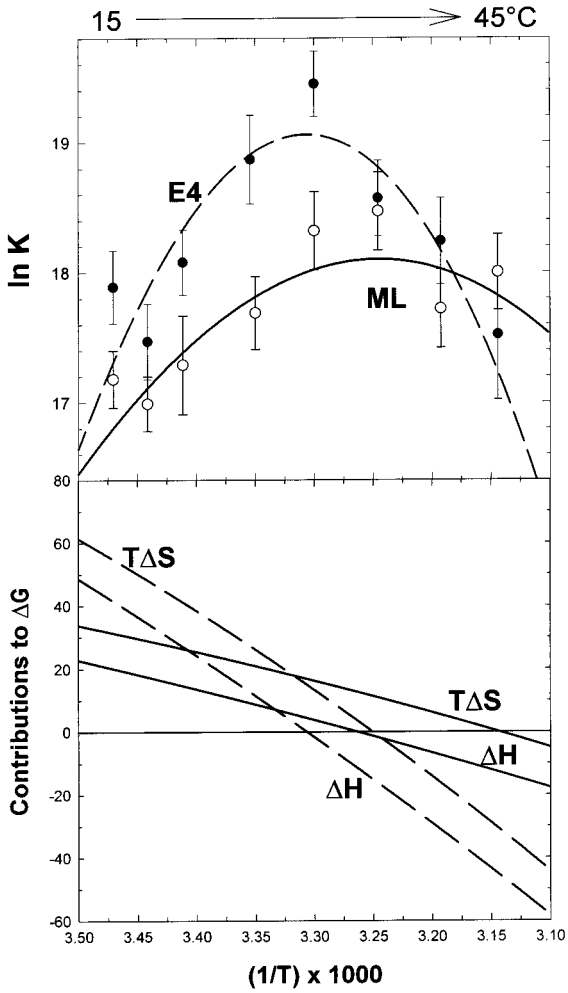

FIGURE 3: van't Hoff analysis of the binding of TBP to the Major Late (○) and E4 (●) promoters. The solid lines depict the values of $\Delta C_p°$ (Table 2) determined as described previously (*17*) from the global best fit of the binding isotherms. The differences in the present E4 data and that published previously result from the inclusion of additional data sets in this analysis. At least two (and in most cases three or more) independently determined isotherms were obtained at each temperature; the value of ln K and confidence limits reported for each data point represent the global analysis of these isotherms.

Table 2: The Temperature Dependence of TBP Binding to the E4 and Major Late Promoters

promoter	$\Delta C_p°$ (kcal/mol K)[a]	T_H °C	T_S °C	$\sqrt{var}$
K_{eq}				
E4: TATATATA	-2.9 ± 0.3	29.3 ± 0.5	34.5 ± 0.7	0.125
MLP: TATAAAAG	-1.1 ± 0.3	33.3 ± 0.8	45.0 ± 1.7	0.139
k_a				
E4	-3.3 ± 0.7	31.8 ± 0.6	34.2 ± 0.8	0.322
MLP	-1.0 ± 0.3	39.7 ± 1.5	47.9 ± 2.5	0.209

[a] $\Delta C_p°$ was calculated following ref *18* as described (*17*).

the error in the measurements. Approximately 80% of the [KCl] dependence of TBP binding is accounted for in the rate of association in a TATA sequence-independent fashion.

In our previous study (*17*), a two-step model was assumed (*20*), and limits to the constant K_B, describing the postulated initial rapid equilibrium, and k_2, the rate constant for the unimolecular isomerization of the second step of the reaction, were derived from the highest TBP concentrations analyzed. Since subsequent FRET studies did not reveal evidence of

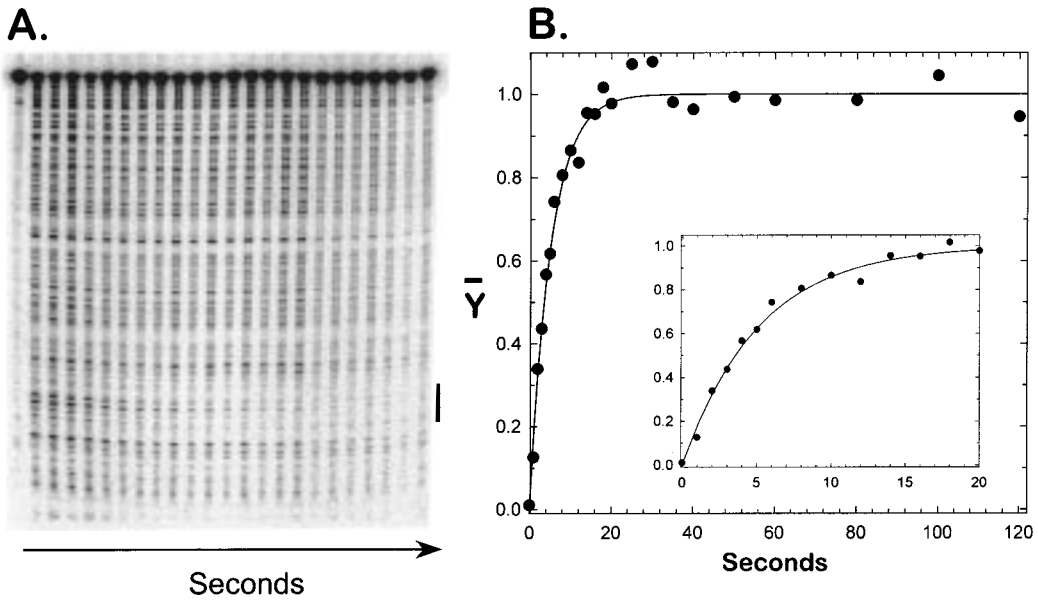

FIGURE 4: (A) The phosphor storage plate image of the gel electrophoretogram of a quench-flow DNase I footprint experiment conducted at 100 mM KCl and 30 °C using 400 nM TBP and DNA containing the E4 promoter. The solid bar on the right side of the gel denotes the TATA box. The density scale of the digital image was compressed 16−8 bits using the default parameters of the ImageQuant software in order to generate this picture; densitometry was conducted on the 16 bit image. (B) The progress curve derived from the experiment shown in A. Each data point corresponds to the lane in A for increasing reaction time left to right. The solid line depicts the best fit to eqs 1 and 3 with $k_{obs} = 0.2 \pm 0.02$ s^{-1}. The overall second-order rate constant is $k_a = 4.9\ (\pm 0.6) \times 10^5$ M^{-1} s^{-1} assuming that $k_d = 0$. The insert is an expanded view of the first 20 s of the reaction.

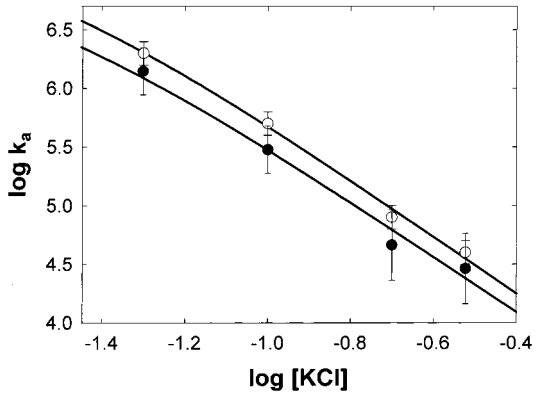

FIGURE 5: The salt dependence of the rate of association of TBP with the Major Late (○) and E4 (●) promoters. The data were fit for Sk_a as described in Figure 2 for the equilibrium binding studies. The results of the fits are shown in Table 1.

the postulated diffusion-limited intermediate (*22*), we have re-explored this question with more extensive data sets for both the Major Late and the E4 promoters. Figure 6 plots k_{obs} versus [TBP] at 100 mM KCl and 20, 30, and 35 °C. All of the data sets are adequately described by the linear dependence of k_{obs} on [TBP] predicted by bimolecular association. Unique values of K_B and k_2 could not be determined by global fitting of the progress curves to the two-step model (data not shown).

The temperature dependence of the association rate of TBP for the Major Late promoter closely matches that of the equilibrium binding constant (Figure 7A); this result was previously observed for the E4 promoter (*17*) and thus, appears to be a general characteristic of TBP−promoter interactions. This characteristic of the association reaction is reflected in the significantly different values of $\Delta C_p°$ for the two promoters that are comparable to the $\Delta C_p°$ values calculated for the equilibrium binding reaction (Table 2). The Major Late promoter presents a lower activation barrier to TBP binding than does the E4 promoter (Figure 7A). A consequence of the correspondence of K_{eq} and k_a is that the calculated values of k_d ($K_{eq} = k_a/k_d$) are independent of temperature within the experimental error propagated from the experimentally determined values of K_{eq} and k_a (Figure 7B).

DISCUSSION

The binding of proteins to DNA is dominated by noncovalent interactions; therefore the experimentally determined equilibrium and kinetic rate constants are dependent upon solution conditions such as temperature, pH, and ion composition and concentration. These dependencies can thus be used to probe the energetic driving forces and mechanisms of a reaction under consideration. The direct comparison of the thermodynamics and association kinetics of TBP binding to the E4 and Major Late promoters provides a foundation for the development of structure−function correlations describing TBP−DNA interactions.

The binding isotherms obtained for the TBP-Major Late promoter interaction at [KCl] ≥ 50 mM are described by the Langmuir polynomial (Figure 1). This result was previously obtained with the E4 promoter (*17*) and appears to be general with regard to the TATA sequence. At physiological salt concentrations, the TBP−DNA isotherms that have been determined are consistent with the binding of a single TBP molecule to a TATA box and do not reflect contributions from either cooperative or self-association reactions. In contrast, at [KCl] < 50 mM (at 30 °C) isotherms determined for the binding of TBP are sigmoidal, displaying positive cooperativity; the mechanism underlying this apparent cooperativity at low ionic strength is unknown.

These results are consistent with analytical ultracentrifugation studies (*30*, *31*) that provide direct evidence demonstrating that *S. cerevisiae* TBP is monomeric at the nano-

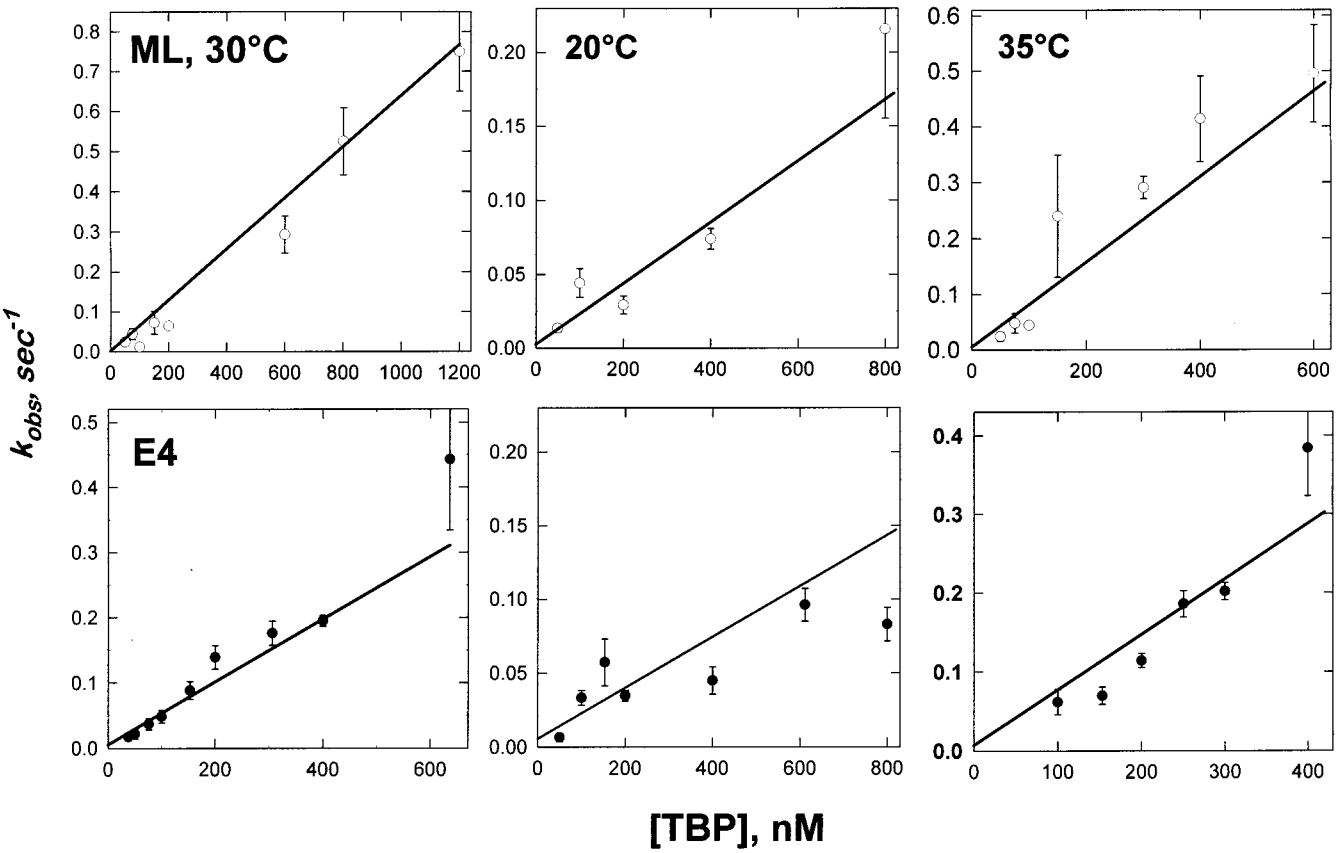

FIGURE 6: The association rate, k_{obs}, determined as a function of TBP concentration for the Major Late (○) and E4 (●) promoters at 20, 30, and 35 °C. The Major Late promoter is shown across the top at the indicated temperatures. The E4 promoter is below. The second-order rate constants, k_a, determined by global analysis of the progress curves are $2.1 \pm 0.3 \times 10^5$ (20 °C), $5.0 \pm 0.8 \times 10^5$ (30 °C), and $9.3 \pm 1.3 \times 10^5$ (35 °C) for the Major Late promoter and $1.3 \pm 0.3 \times 10^5$ (20 °C), $4.7 \pm 0.4 \times 10^5$ (30 °C), and $7.2 \pm 1.1 \times 10^5$ (35 °C) for the E4 promoter.

molar concentrations present in these and previously published equilibrium binding and kinetics studies (*17*, *20*−*22*). The ultracentrifugation studies also demonstrate that self-association of *S. cerevisiae* TBP to tetramers and octamers occurs at micromolar concentrations under these experimental conditions. For human TBP, dimerization competitive with DNA binding has been reported with a K_d of 5 nM (*32*, *33*) under experimental conditions different than those used in our studies. If such a reaction were present in our *S. cerevisiae* TBP studies with a K_d comparable to that of DNA binding, this linked equilibrium would be evident by TBP−DNA binding isotherms less steep than the Langmuir polynomial (i.e., "anti-cooperative") since the concentration of TBP monomers would not increase linearly with the total TBP over the concentration ranges analyzed. This phenomenon was not observed at any of the solution conditions that have been analyzed.

In addition, the slow dissociation of the human TBP dimers was demonstrated to limit the rate of DNA binding by TBP (*32*, *33*). A TBP self-association reaction competitive with DNA binding will be reflected in the observed rate of binding and can yield a nonlinear dependence of k_{obs} on [TBP] if the K_d of dimerization is comparable to the protein concentration range being studied. The data shown in Figure 6 span as great as 3 orders of magnitude in TBP concentration and provide no evidence for a coupled competitive dimerization reaction. Thus, the equilibrium and kinetics studies of TBP−DNA binding and the analytical ultracentrifugation studies of self-association of *S. cerevisiae* TBP are all consistent with the model of *S. cerevisiae* TBP-promoter binding of TBP + TATA ↔ TBP−TATA used to interpret our studies. The reported properties of the TBP−promoter interaction reflect complex formation between monomeric TBP and DNA.

A TBP−TATA binding mechanism has been proposed (*22*) in which the slower than diffusion-limited kinetics observed for TBP is due to the extremely *unfavorable* quasi-equilibrium for the formation of a productive encounter complex of DNA and TBP. No diffusion-limited intermediate was detectable in kinetics studies on time scales as short as several milliseconds. This mechanism contrasts to a two-step model where a stable diffusion-limited TBP−DNA intermediate isomerizes to the final complex (*28*). While values of K_B and k_2 were estimated in the context of the two-step model from our initial quench-flow footprinting studies (*17*), the linear increase in k_{obs} with [TBP] for both promoter sequences at all temperatures does not justify application of this mechanism to these data. Thus, for both promoter sequences, the "slow binding" of TBP results from the high activation barrier for the formation of a productive encounter complex (*22*).

Salt-dependent effects on DNA−ligand interactions are the consequence of the charged nature of the DNA and its interaction with the surrounding counterions; a substantial concentration of positively charged counterions accumulates in the vicinity of the DNA to reduce its axial charge density and strongly influences protein-binding reactions. The identical [KCl] dependencies of equilibrium binding of TBP

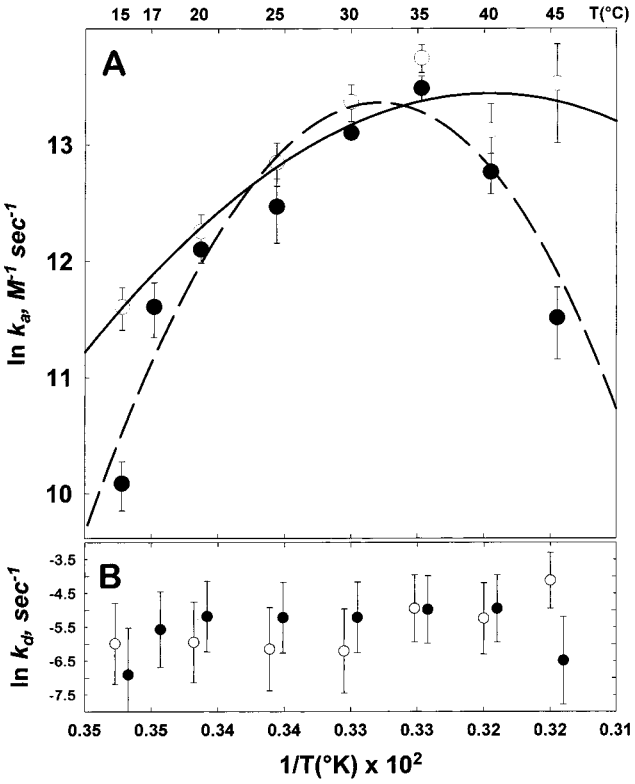

FIGURE 7: (A) Arrhenius plot of the second-order rate constants, k_a, for the binding of TBP to the Major Late (○) and E4 (●) promoters. The lines denote the best fits for values of $\Delta C_p°$ tabulated in Table 2 as in Figure 3. (B) Values of the kinetic dissociation constant calculated from the relationship $K_{eq} = k_a/k_d$. The errors on the experimentally determined values of K_{eq} and k_a were propagated to generate the estimated errors on the calculated values of k_d.

to the E4 and Major Late promoters suggest that identical electrostatic interactions are formed within the protein-DNA complexes and that structurally similar interfaces are present. The salt-dependent effects on the interaction of TBP with the two promoters are roughly consistent with the number of ion pairs that can be inferred from the crystallographic studies. These data are consistent with the geometry of the TBP complexes with the E4 and Major Late promoters being comparable in solution.

However, the different temperature dependencies of TBP binding to the two promoter sequences do point to energetic differences unrelated to the overall geometry of the complexes. Hydroxyl radical footprinting studies of TBP−promoter complexes conducted under these experimental conditions (unpublished data) show no evidence of heterogeneity in the positioning of TBP on the TATA box sequences (*34*). DNase I footprinting is not sensitive to the observed bidirectional orientation of TBP on TATA box sequences (*34*). Since the orientation distribution on the Major Late and *CyC1* promoters is equivalent (the TATATAAA *CyC1* sequence differs from the E4 sequence only in position 7), it is unlikely that TBP orientation is the source of the observed promoter-dependent thermodynamic and kinetic differences in binding.

The calculated values of T_H and T_S (the temperatures at which the $\Delta H°$ and $\Delta S°$ are 0, respectively; Table 2) show that the TBP−E4 interaction is entropically driven at low temperature and enthalpically driven at high temperature. In contrast, the TBP−Major Late promoter is entropically driven ($T\Delta S°$ is positive) over virtually the entire temperature range investigated with $\Delta H°$ less positive compared to the formation of the TBP−E4 complex. The $\Delta C_p°$ value of -1.1 ± 0.3 determined for the Major Late promoter is significantly lower than that determined for the E4 promoter (Table 2). This value is only 2-fold more negative than the $\Delta C_p°$ of −0.5 kcal/(M K) calculated from the burial of nonpolar surface area in the *S. cerevisiae* TBP−DNA cocrystal structure (*13*). The different $\Delta C_p°$ values were unanticipated because both promoters bind TBP with high affinity and their cocrystal structures with TBP display only local differences.

A limitation of this comparison with the crystal structures is that the N-terminal domain of *S. cerevisiae* TBP is not present in the crystal and DNA cocrystal structures. While the fluorescence of the single tryptophan in TBP located within the N-terminal domain changes upon DNA binding (*21*), we believe that it is unlikely that a DNA sequence-specific contact of the N-terminal domain accounts for the significantly different temperature dependencies of TBP binding the E4 and Major Late promoters since its presence or absence has little effect on DNA-binding by *S. cerevisiae* TBP (*35*).

The E4 is the most flexible of possible TATA box sequences, composed entirely of TpA base steps, while the Major Late promoter possesses a four base "A tract" that is relatively rigid (*15*). Since the Major Late promoter appears to be an exception to a general trend toward more flexible TATA box sequences binding TBP more tightly, it is possible that it exists in a conformation that is predisposed toward TBP binding. Thus, the more favorable enthalpy of binding the Major Late promoter may be due to its lesser deformation upon complex formation with TBP. Correspondingly, the greater entropy of the flexible alternating TpA sequence of the E4 promoter may account for the decreased T_S relative to the Major Late promoter. These possibilities are being explored through the analysis of TBP−DNA complexes whose cocrystal structures have been solved (S. Burley, personal communication) that possess single-base substitutions within the Major Late promoter sequence. While TpA-rich sequences tend toward more negative values of $\Delta C_p°$, as suggested by the E4 and Major Late promoter data presented herein, structural compensations that accommodate less favorable TATA box sequences appear to play a key role in determining the $\Delta C_p°$ of TBP binding. $\Delta C_p°$ values ranging from 0 to −2.5 kcal/(mol K) have been obtained for TBP−TATA interactions whose $\Delta G°$'s of binding at 30 °C are equivalent within experimental error (A. K. M. M. Mollah, B. Gilden, E. Jamison, and M. Brenowitz, unpublished data). These results are significantly different than those obtained from similar studies of the *Escherichia coli* Lac repressor (*36*).

The effect of the TATA sequence on TBP-induced DNA bending is also of interest with regard to the structure of the TBP−DNA transition state; sequence-specific contacts could form as the DNA bends during the course of the association reaction. However, the fact that DNA binding and bending occurs simultaneously (*22*) argues that the transition-state structure is similar to that of the final complex. Is there additional evidence to support this hypothesis? The relative magnitude of the salt dependence of the association kinetics versus the thermodynamics of a DNA-binding reaction is

expected to be small for a diffusion-limited reaction (*37*) since the association rate is only dependent upon the frequency of collision of the substrates. Electrostatic screening of the macromolecules by ions contributes only slightly to this process. In this case, the ion pairs present in the final complex need not be present in the productive encounter complex that proceeds rapidly down the reaction pathway.

In contrast, the magnitude of the salt dependence of the association kinetics is expected to be large if ions are released or bound at or proceeding the rate-limiting step of the reaction (*37*). A two-step reaction which proceeds via a pre-equilibrium followed by a rate-limiting step behaves in this fashion (*38*). Similarly, the salt dependence of the rate of TBP−DNA association is consistent with that expected for a non-diffusion-limited reaction. That the TBP−DNA transition state detectable by DNase I footprinting has an appreciable character of the final complex is indicated by the observation that ∼80% of the salt dependence of binding is present in the association rate constant (Table 1). The identical [KCl] dependencies of k_a for the two promoters suggest that they bind TBP through a similar initial reaction step. This observation is consistent with the hypothesis that TBP "samples" the DNA population for the particular conformation "predisposed" to adopt the distorted structure of the complex (*22*) and, thus, that the transition state possesses most of the structural and energetic features of the final complex.

The identity of the $\Delta C_p°$ values calculated from the van't Hoff and Arrhenius analyses for TBP binding to the E4 and Major Late promoters (Table 2) also suggests that the transition state of the reaction is comparable to the final complex. A consequence of this result is that the kinetic dissociation constants are predicted to be invariant with temperature for both promoters. While nonlinear Arrhenius plots are often evidence that a reaction proceeds via a multistep mechanism (e.g., refs *39*, *40*) single step reactions can also display curved Arrhenius plots if there is a $\Delta C_p°$ associated with either the ground state of the reaction or the transition-state complex (*41*, *42*). For example, the folding kinetics of T4 lysozyme and trypsin is characterized by $\Delta C_p°$ values comparable to those determined for the folding equilibrium (*43*−*46*); these results were interpreted to reflect that the structure of the transition state is close to that of the native state. Further thermodynamics and kinetis studies of the temperature dependence of TBP binding as a function of TATA box sequence are in progress to resolve this issue.

The differences observed in the response of these two highly efficient promoters to an environmental variable suggest that the variation in TATA sequence observed at promoters may not be simply to modulate affinity (*47*), but may play a more subtle role in the regulation of transcription initiation. Similarly, such differences may contribute to the cooperative interaction of TBP with other transcription factors (*48*). These DNA sequence differences might be expected to be reflected in the kinetic mechanism of TBP binding. Indeed, FRET studies indicate that after the formation of the productive encounter complex there exists a complex reaction pathway that is TATA sequence-dependent (*49*, *50*). Thus, despite the detailed pictures that have been obtained of TBP−TATA complexes, much remains to be learned about the pathways through which these complexes form. The coordinated application of footprinting and FRET to the thermodynamics and kinetics of TBP−DNA interactions together with analytical ultracentrifugation analysis of its self-association properties is beginning to reveal the chemistry underlying the function of a protein that is essential in all eukaryotic cells.

ACKNOWLEDGMENT

We thank Robyn Moir, Lawrence Parkhurst, Kay Parkhurst, and Ian Willis for helpful discussions and critical readings of the manuscript.

REFERENCES

1. Sharp, P. A. (1992) *Cell 68*, 819−821.
2. Rigby, P. W. J. (1993) *Cell 72*, 7−10.
3. McKnight, S. (1996) *Genes Dev. 10*, 367−381.
4. Hernandez, N. (1993) *Genes Dev. 7*, 1291−1308.
5. Burley, S. K., and Roeder, R. G. (1996) *Annu. Rev. Biochem. 65*, 760−799.
6. Smale, S. T. (1994) in *Transcription: Mechanisms and Regulation* (Conaway, R. C., and Conaway, J. W., Eds.) pp 63−81, Ravne Press, NY.
7. Wong, J. M., and Bateman, E. (1994) *Nucleic Acids Res. 22*, 1890−1896.
8. Nikolov, D. B., Hu, S.-H., Lin, J., Gasch, A., Hoffman, A., Horikoshi, M., Chua, N.-H., Roeder, R. G., and Burley, S. K. (1992) *Nature 360*, 40−46.
9. Chasman, D. I., Flaherty, K. M., Sharp, P. A., and Kornberg, R. D. (1993) *Proc. Natl. Acad. Sci. U.S.A. 90*, 8174−8178.
10. Nikolov, D. B., and Burley, S. K. (1994) *Nat. Struct. Biol. 1*, 621−637.
11. DeDecker, B. S., O'Brien, R., Fleming, P. J., Geiger, J. H., Jackson, S. P., and Sigler, P. B. (1996) *J. Mol. Biol. 264*, 1072−1084.
12. Kim, J. L., Nikolov, D. B., and Burley, S. K. (1993) *Nature 365*, 520−527.
13. Kim, Y., Geiger, J. H., Hahn, S., and Sigler, P. B. (1993) *Nature 365*, 512−520.
14. Kim, J. L., and Burley, S. K. (1994) *Nat. Struct. Biol. 1*, 638−653.
15. Juo, Z. S., Chiu, T. K., Leibermann, P. M., Baikalov, I., Berk, A. J., and Dickerson, R. E. (1996) *J. Mol. Biol. 261*, 239−254.
16. Nikolov, D. B., Chen, H., Halay, E. D., Hoffman, A., Roeder, R. G., and Burley, S. K. (1996) *Proc. Natl. Acad. Sci.U.S.A. 93*, 4862−4867.
17. Petri, V., Hsieh, M., and Brenowitz, M. (1995) *Biochemistry 34*, 9977−9984.
18. Ha, J.-H., Spolar, R. S., and Record, M. T., Jr. (1989) *J. Mol. Biol. 209*, 801−816.
19. Spolar, R. S., and Record, M. T., Jr. (1994) *Science 263*, 777−784.
20. Hoopes, B. C., LeBlanc, J. P., and Hawley, D. K. (1992). *J. Biol. Chem. 267*, 11539−11547.
21. Perez-Howard, G. M., Weil, T., and Beechem, J. M. (1995) *Biochemistry 34*, 8005−8017.
22. Parkhurst, K. M., Brenowitz, M., and Parkhurst, L. J. (1996) *Biochemistry 35*, 7459−7465.
23. Sawadogo, M., and Roeder, R. G. (1985) *Proc. Natl. Acad. Sci. U.S.A. 82*, *4394*−*4398*.
24. Hsieh, M., and Brenowitz, M. (1996) *Methods Enzymol. 274*, 478−492.
25. Brenowitz, M., Senear, D. F., Shea, M. A., and Ackers, G. K (1986) *Methods Enzymol. 130*, 132−181.
26. Brenowitz, M., Senear, D. F., Jamison, E., and Dalma-Weiszhaus, D. D. (1993) in *Footprinting Techniques for Studying Nucleic Acids-Protein Complexes* (Revzin, A., Ed.) pp 1−43, Academic Press, New York.
27. Hill, A. V. (1913) *Biochem. J. 7*, 471−480.
28. Strickland, S., Palmer, G., and Massey, V. (1975) *J. Biol. Chem. 250*, 4048−4052.

29. Record, M. T., Jr., DeHaseth, P., and Lohman, T. M. (1977) *Biochemistry 16*, 4791−4796.
30. Daugherty, M. A., Brenowitz, M., and Fried, M. G. (1998) *Biophys. J. 74*, A74.
31. Daugherty, M. A., Brenowitz, M., and Fried, M. G. (submitted for publication).
32. Coleman, R. A., Taggart, A. K. P., Benjamin, L. R., and Pugh, B. F. (1995) *J. Biol. Chem. 270*, 13842−13849.
33. Coleman, R. A., and Pugh, B.F. (1997) *Proc. Natl. Acad. Sci. U.S.A. 94*, 7221−7226.
34. Cox, J. M., Hayward, M. M., Sanchez, J. F., Gegnas, L. D., van der Zee, S., Dennis, J. H., Sigler, P. B., and Schepartz, A. (1997) *Proc. Natl. Acad. Sci. U.S A. 94*, 13475−13480.
35. Kuddus, R., and Schmidt, M. C. (1993) *Nucleic Acids Res. 21*, 1789−1986.
36. Frank, D. E., Saecker, R. M., Bond, J. P., Capp, M. W., Tsodikov, O. V., Melcher, S. E., Levandoski, M. M., and Record, M. T., Jr. (1997) *J. Mol. Biol. 267*, 1186−1206.
37. Lohman, T. M. (1985) *CRC 19*, 191−245.
38. Roe, J.-H., Burgess, R. R., and Record, T. M., Jr. (1984) *J. Mol. Biol. 176*, 495−521.
39. Takagi, Y., and Taira, K. (1995) *FEBS Lett. 361*, 273−275.
40. Oliveberg, M., and Fersht, A. (1996) *Biochemistry 35*, 2738−2749.
41. Oliveberg, M., Tan, Y.-J., and Fersht, A. (1995) *Proc. Natl. Acad. Sci. U.S.A. 92*, 8926−8929.
42. Schindler, T., and Schmid, F. X. (1996) *Biochemistry 35*, 16833−16842.
43. Segawa, S., and Sugihara. (1984) *Biopolymers 23*, 2473−2499.
44. Pohl, F. M. (1968) *Eur. J. Biochem. 7*, 146−152.
45. Chen, B., and Schelmann, J. A. (1989) *Biochemistry 28*, 685−691.
46. Chen, B., Baase, W. A., and Schelmann, J. A. (1989) *Biochemistry 28*, 691−699.
47. Meyer, T., Carlstedt-Duke, J., and Starr, D. B. (1997) *J. Biol. Chem. 272*, 30709−30714.
48. Librizzi, M. D., Brenowitz, M., and Willis, I. (1998) *J. Biol. Chem. 273*, 4563−4568.
49. Parkhurst, K., Richards, R., Brenowitz, M., and Parkhurst, L. J. (1998) *Biophys. J. 74*, A150.
50. Parkhurst, K., Richards, R., Brenowitz, M., and Parkhurst, L. J. (manuscript in preparation).

BI981072U